DEUTSCHES ELEKTRONEN-SYNCHROTRON DESY

DESY 71/7
February 1971

Elastic Electron-Deuteron Scattering and the Electric Neutron Form Factor at Four Momentum Transfers $5\ \text{Fermi}^{-2} < q^2 < 14\ \text{Fermi}^{-2}$

by

S. Galster, H. Klein, J. Moritz, K. H. Schmidt, D. Wegener
Institut für Experimentelle Kernphysik der Universität (TH)
und des Kernforschungszentrums Karlsruhe

and

J. Bleckwenn
Deutsches Elektronen-Synchrotron DESY, Hamburg

2 HAMBURG 52 · NOTKESTIEG 1

Elastic Electron-Deuteron Scattering and the Electric Neutron Formfactor at Four Momentum Transfers $5\ \text{Fermi}^{-2} < q^2 < 14\ \text{Fermi}^{-2}$

S. Galster, H. Klein, J. Moritz, K.H. Schmidt, D. Wegener

Institut für Experimentelle Kernphysik der Universität (TH)

und des Kernforschungszentrums Karlsruhe

J. Bleckwenn

Deutsches Elektronen-Synchrotron DESY, Hamburg

Summary

The cross section for elastic electron-deuteron scattering was measured for ten four-momentum transfers squared in the range

$$5\ f^{-2} < q^2 < 14\ f^{-2}$$

From the measured cross sections the sum $A(q^2)$ of charge and quadrupole form factors was determined.

The experimental values are compared with theoretical predictions including relativistic corrections. Different deuteron wave functions and different parametrizations for the electric neutron form factor G_{EN} were used. The best fit to the experimental data was found with the wave function of Feshbach-Lomon and the parametrization

$$G_{EN}(q^2) = - \frac{\mu_N \tau}{1+5.6\tau} G_{EP}(q^2) \ , \qquad \tau = \frac{q^2}{4M^2}$$

Introduction

Experimental measurements of the deuteron form factors are necessary to describe electromagnetic processes on the deuteron. Three form factors can be assigned to the deuteron[1,2]. In the static limit, they correspond to the charge, the quadrupole and the magnetic moment. In Born approximation, the differential cross section for elastic electron-deuteron scattering is found to have the following form[3]:

$$\frac{d\sigma}{d\Omega} = \left(\frac{d\sigma}{d\Omega}\right)_{Mott} \cdot \{A(q^2) + B(q^2)tg^2(\Theta/2)\} \qquad (1)$$

$A(q^2)$ and $B(q^2)$ contain the three form factors of the deuteron. For electron scattering angles smaller than 15^o the second term contributes less than 0.1 % to the cross section and can be neglected. $A(q^2)$ is determined by the sum of charge and quadrupole form factors, the magnetic form factor contributing less than 5 % to $A(q^2)$.

Moreover, if one takes into account that the deuteron consists of a neutron and a proton, elastic electron-deuteron scattering[4-11] supplies the deuteron wave function in the range of small nucleon distances and the sum of the electric form factors of the nucleons.

The scattering on both nucleons is coherent, and only the isoscalar part of the electromagnetic interaction contributes to the cross section since the isospin T of the deuteron equals zero. For electron scattering angles smaller than 15^o, the following relation applies in good approximation:

$$\frac{d\sigma}{d\Omega} \propto \{G_{EN}(q^2) + G_{EP}(q^2)\}^2 \qquad (2)$$

If the electric form factor G_{EP} of the proton and the deuteron wave function can be considered to be known, the sign and the magnitude of the electric neutron form factor G_{EN} can be determined. Fortunately, the cross section depends sensitively on the neutron form factor (Fig. 1), while it is a disadvantage that the calculated cross section is influenced very strongly by the wave function used (Table I).

The behavior of the nucleon interaction for small distances is known essentially from nucleon-nucleon scattering experiments[12] in which the center-of-mass energy of the nucleon system increases with the four-momentum transfer. Elastic electron-deuteron scattering allows in addition the investigation of the nucleon-nucleon interaction for low center-of-mass energies which are independent of the four-momentum transfer. Since the isoscalar part of the electric form factor of the nucleon is included in the cross section as a further independent parameter, measurements must be carried out for different four-momentum transfers to separate the influence of the wave function.

In this work, the differential cross section for elastic electron-deuteron scattering was measured for three four-momentum transfer intervals[13]. Until now, two previous measurements have been performed in the range of four-momentum transfer investigated in this study[7,10].

Other possible methods allowing to determine the electric neutron form factor are the quasielastic electron-deuteron scattering and the π^+-electro-production on hydrogen in the backward direction. In both cases an extrapolation in the Mandelstam variable u to the neutron pole is desirable, moreover theoretical assumptions make the analysis uncertain.

Theoretical formula for the deuteron cross section

Formulae for calculating the cross section for elastic electron-deuteron scattering have been derived by various authors[15-19]. The results differ in their ansatz for the deuteron current. The contribution of meson exchange current[14] is neglected. Gourdin[16] derived the following formula:

$$\frac{d\sigma}{d\Omega} = \left(\frac{d\sigma}{d\Omega}\right)_{Mott}\left\{G_C^2(q^2)+\frac{8}{9}\eta^2 G_Q^2(q^2)+\frac{2}{3}\eta(1+\eta)G_M^2(q^2)\left(1+2(1+\eta)tg^2(\Theta/2)\right)\right\} \tag{3}$$

$$= \left(\frac{d\sigma}{d\Omega}\right)_{Mott}\left\{A(q^2) + B(q^2)tg^2(\Theta/2)\right\}$$

$$A(q^2) = G_C^2(q^2) + \frac{8}{9}\eta^2 G_Q^2(q^2) + \frac{2}{3}\eta G_M^2(q^2)(1+\eta)$$

$$B(q^2) = \frac{4}{3}\eta(1+\eta)^2 G_M^2(q^2) \tag{4}$$

$$\eta = \frac{q^2}{4M_D^2}$$

$$G_C = 2\, G_{ES}\cdot C_E$$

$$G_Q = 2\, G_{ES}\cdot C_Q \tag{5}$$

$$G_M = \frac{M_D}{M_P}\left(2G_{MS}C_S + G_{ES}C_L\right)$$

G_{ES} and G_{MS} are the isoscalar electric and magnetic form factor of the nucleon:

$$G_{ES} = \frac{1}{2}\left(G_{EP} + G_{EN}\right)$$

$$G_{MS} = \frac{1}{2}\left(G_{MP} + G_{MN}\right) \tag{6}$$

C_E, C_Q, C_S, C_L describe the deuteron structure and can be calculated in good approximation from the non-relativistic deuteron wave function u(r) for the S-state and w(r) for the D-state:

$$C_E = \int \{u^2(r) + w^2(r)\}\, j_o(\tfrac{qr}{2})\, dr$$

$$C_Q = \frac{3}{\sqrt{2}\eta} \int w(r)\, \{u(r) - \frac{w(r)}{\sqrt{8}}\}\, j_2(\tfrac{qr}{2})\, dr$$

$$C_L = \frac{3}{2} \int w^2(r)\, \{j_o(\tfrac{qr}{2}) + j_2(\tfrac{qr}{2})\}\, dr \qquad (7)$$

$$C_S = \int \{u^2(r) - \frac{w^2(r)}{2}\}\, j_o(\tfrac{qr}{2})\, dr$$

$$+ \frac{1}{\sqrt{2}} \int w(r)\, \{u(r) + \frac{w(r)}{\sqrt{2}}\}\, j_2(\tfrac{qr}{2})\, dr$$

$j_o(\frac{qr}{2})$ and $j_2(\frac{qr}{2})$ are spherical Bessel functions.

In Fig. 2, the theoretical predictions[16] of the electric part G_C^2, the quadrupole part $\frac{8}{9}\eta^2 G_Q^2$, and the magnetic part $\frac{2}{3}\eta G_M^2$ of $A(q^2)$ and their sum have been plotted as a function of the four-momentum transfer. In this calculation the dipole-fit

$$G_{EP} = (1 + \frac{q^2}{0.71})^{-2} \quad , \qquad q^2 \text{ in } (\text{GeV/c})^2 \qquad (8)$$

and the scaling law

$$G_{MP} = \mu_P \cdot G_{EP} \quad , \qquad \mu_P = 2.79278$$

$$G_{MN} = \mu_N \cdot G_{EP} \quad , \qquad \mu_N = -1.91315 \qquad (9)$$

for the nucleon form factors and the Hamada-Johnston[20] wave function were used. The electric neutron form factor was set equal to zero. Obviously, the electric and the quadrupole form factor give the main contribution to

$A(q^2)$ in the range of four-momentum transfer covered by this experiment.

Relativistic corrections to these formulae which take into account the deformation of the wave function for a moving deuteron, have been given by Gross[19]. Since the magnetic part is less than 5 % in the entire range investigated, these corrections were applied only to the charge and quadrupole scattering. In Fig. 3 these relativistic corrections have been plotted as a function of q^2, where the same parameters have been used as in Fig. 2. The relativistic corrections are smaller than 10 % throughout the entire range investigated.

Experimental Setup and Method of Measurement

The experiment was performed at DESY with the slow ejected electron beam incident on a 3 cm diameter liquid deuterium condensation target[+)][21]. The equipment for the detection of the scattered electrons and the recoil deuterons (Fig. 4) is mounted on two platforms pivoting horizontally around the target.

The scattered electrons are analysed with a spectrometer which consists of a magnet[++)] with a homogenous field, four wire spark chambers and a scintillation counter setup. The counter setup, consisting of three scintillation and one shower counter, separates electrons from other particles. A coincidence signal of these counters defines a scattering event. The electrons are deflected in the magnetic field perpendicular to the scattering plane. Their trajectories are determined by means of the wire spark chambers behind the magnet. For calculating the radius of curvature, the center of the target is taken as the origin of the scattering process.

+) Dupont H-foil, 0.05 mm

++) DESY MB standard magnet

With a mean deflection angle of 16.5 degrees, the momentum resolution of the spectrometer is ±0.6 %. With a maximum magnetic field of 22.4 kGauss, electrons can be analyzed up to a momentum of 3.7 GeV/c. The measurements are carried out with an average radius of the electron trajectories of 3.5 m and an aperture angle in the deflection plane of 1.6 degrees. A momentum range of ± 20 % is covered with a constant solid angle of 0.68 msterad. The scattering angle is known with an accuracy of ± 0.6 mrad for each scattering event.

The spark chambers[22] have a sensitive area of 256 x 512 mm^2 with a 6 mm electrode gap and a ferrite core readout on the ground and high voltage sides. This allows to measure two coordinates simultaneously with one spark chamber. 120 nsec after the passage of a particle, a spark gap is ignited. It applies a 6 kV pulse of 200 nsec duration to the four spark chambers. With a clearing voltage of 50 V dc, the sensitive time of the chamber system is 500 nsec. The average detection probability ε_K = (96-99) % of one chamber was attained with a gas mixture of 85 % Neon, 10 % Helium and 5 % Argon. An event is evaluated only if the centroids of the sparks of three or four chambers give a straight line in both projections. The detection probability for these straight lines is 98 %.

The recoil deuterons are detected with a scintillation counter (Fig. 4) which has an area of 200 x 200 mm^2 placed on the second platform. This deuteron-counter is 10 mm thick, which is sufficient to separate deuterons from other particles by pulse height analysis.

Spark chamber readout- and counter electronic system[+)] are connected to a computer CDC 1700[23] by an interface. The computer records the following data and stores them on magnetic tape:

(1) Centroids of coordinates of all sparks in the four spark chambers

(2) Pulse height of the electron shower counter

(3) Pulse height of the deuteron-counter

(4) Contents of electronic scalers

Results and Corrections

The following criteria were used to select those events from the total data stored on magnetic tape which are assigned to the elastic electron-deuteron scattering:

a) The deuteron-counter has detected a particle in coincidence with the electron.

b) The pulse height in the deuteron-counter is higher than the threshold set by the specific energy loss of a deuteron in the scintillator material.

Fig. 5 shows the measured pulse height spectrum demonstrating clearly the separation of protons and deuterons. In Table II the energy losses of protons and deuterons in plastic material[24] are shown. They confirm the experimental result.

+) Chronetics 100 mc/s electronics
Le Croy analog-digital converter
Borer electronic scalers

Using these criteria, energy spectra of scattered electrons were obtained which are shown in Fig. 6, they demonstrate the possibility to separate the elastic scattering process from the quasielastic scattering process $e + d \rightarrow e + p + n$. For a quantitative separation of the two processes a minimization program[+)] was used to fit two curves to the measured data. The curves were obtained by folding the radiative tail of the elastic and quasielastic scattering process with a Gaussian function which reflects the finite energy resolution of the electron spectrometer. Formulae by Bartl and Urban[25] were taken for the calculation of the radiative tail, but higher approximations for the relation between the missing energy ΔE in the electron spectrum and the energy of photons from inner bremsstrahlung were used. The fitted curves describe the measured data well.

The number of elastic scattering events obtained in this way is plotted in Fig. 7 as a function of the threshold in the pulse height spectrum of the deuteron-counter. The horizontal section of the curve shows that no elastic events are lost as a result of fixing threshold in the pulse height spectrum.

With our experimental setup the particle trajectories can be traced back into the target and the electron scattering angle is known exactly for each scattering event. This property has been used to determine the counting rate in intervals of the scattering angle of 0.4° (Fig. 8). In this way, cross sections $d\sigma/d\Omega$ can be given which have been averaged over small intervals of the four-momentum transfer squared.

+) Minuit, CERN

The measured counting rates were corrected for the efficiencies of the counters and the spark chamber spectrometer. In addition, the radiative corrections[26] were applied. Table III contains a compilation of the corrections and their errors. In Table IV the differential cross sections obtained from our measurements have been listed, and Table V contains a compilation of the total errors of the measurements. It is useful to separate the Mott cross section and to give only the deuteron form factor $A(q^2)$ according to formula (1). The values of $A(q^2)$ and their errors are compiled in Table VI.

In Fig. 9 the measured form factors $A(q^2)$ together with those obtained by other authors[4-11] are shown. The results of this experiment fit a curve passing through the values measured in previous investigations. Moreover the experimental form factors are compared with theoretical values which are obtained by using the theory of Gross[19], the four pole fit[27] for the electric proton form factor G_{EP}, the scaling law formula (9) and different deuteron wave functions[20,28-30]. In this figure the electric neutron form factor G_{EN} is assumed to be zero. The experimental values differ from the theoretical ones, i.e. the assumption of $G_{EN} = 0$ gives no agreement. Therefore in Fig. 10 theoretical values of $A(q^2)$ are shown with the electric neutron form factor G_{EN} being varied in the region $G_{EN} = -0.05$ to $G_{EN} = +0.05$, using the wave function of Hamada-Johnston.

To get an idea of the best analytical expressions for G_{EN}, we have computed χ^2 by comparing the experimental values of $A(q^2)$ with theoretical predictions using different wave functions and different parametrizations for G_{EN}. The results are listed in Table VII for the following analytical expressions

$$G_{EN} = 0 \tag{10 a}$$

$$G_{EN} = -\mu_N \tau G_{EP} \tag{10 b}$$

$$G_{EN} = -\mu_N \frac{\tau}{1+4\tau} G_{EP} \tag{10 c}$$

$$G_{EN} = -\mu_N \frac{\tau}{1+p\tau} G_{EP} \tag{10 d}$$

$$\tau = \frac{q^2}{4M^2}$$

Equation (10 b) is the result of a calculation based on O(4,2) symmetry properties[31]. Equation (10 c) is an adhoc ansatz[32]. Moreover, we have fitted the formula 10 d, p being a free parameter.

Values of $\chi_F^2 \approx 1$ (Table VII) were only obtained for the wave functions of McGee, Hamada-Johnston and Feshbach-Lomon and the ansatz (10 d). The values for G_{EN} calculated by using those wave functions are shown in Fig. 11-13, they are equal within the error limits and show a systematic deviation from zero. The uncertainties in the values of the proton form factor are not included in the calculated errors of the neutron form factor. Taking them into account would enlarge the error bars by a factor of 1.5 to 2.

To give results which are independent of the uncertainties in the proton form factor Table VIII summarizes the measured values of the isoscalar nucleon form factor

$$G_{ES} = \frac{1}{2} (G_{EP} + G_{EN}) \tag{11}$$

calculated according to formula (5).

Acknowledgments

We are deeply indebted to Professor H. Schopper for his liberal support and to our collaborators Dr. G. Hartwig and Dr. W. Schmidt-Parzefall for assistance during the earlier stages of the experiment.

We wish to thank Professors A. Citron, W. Jentschke, P. Stähelin, M.W. Teucher, G. Weber as well as Dr. H.O. Wüster for their constant interest in this experiment. Further thanks are due to Dr. D. Degèle, Mr. G. Kessler and Mr. H. Kumpfert and their groups and to Mr. D. Rogner, who supported the setup of the experiment at the external beam at the Deutsches Elektronen-Synchrotron Hamburg.

The assistance of Ing. H. Sindt in constructing, testing and carrying out the experiment is gratefully acknowledged. Professor H. Feshbach and Professor E. Lomon kindly provided us with their program for the calculation of the deuteron wave function.

This work was supported by the Bundesministerium für Bildung und Wissenschaft.

References

1. V. Glaser and B. Jaksic, Nuovo Cimento 5, 1197 (1957)
2. V.M. Dubovik and A.A. Cheshkow, Soviet Phys. JETP 24, 111 (1967)
3. T.A. Griffy and L.I. Schiff, High Energy Physics, Vol. I, Burshop
4. J.A. McIntyre and S. Dhar, Phys.Rev. 106, 1074 (1957)
5. J.I. Friedman, H.W. Kendall and P.A. Gram, Phys.Rev. 120, 992 (1960)
6. D.J. Drickey and L.N. Hand, Phys.Rev. Letters 9, 521 (1962)
7. D. Benaksas, D. Drickey and D. Frèrejacque, Phys.Rev. 148, 1327 (1966), Phys.Rev. Letters 13, 353 (1964)
8. B. Grossetête, D. Drickey and P. Lehmann, Phys.Rev. 141, 1425 (1966)
9. E.F. Erickson, Nucleon Structure, edited by R. Hofstadter and L.I. Schiff (Stanford University Press, Stanford, Calif., (1963), p 370)
10. C.D. Buchanan and M.R. Yearian, Phys.Rev. Letters 15, 303 (1965)
11. J.E. Elias, J.I. Friedman, G.C. Hartman, H.W. Kendall, P.N. Kirk, M.R. Sogard and L.P. van Speybroeck, Phys.Rev. 177, 2075 (1969)
12. J. Engler, K. Horn, J. König, F. Mönnig, P. Schludecker, H. Schopper, P. Sievers, H. Ullrich (Karlsruhe) and K. Runge (CERN), Phys. Letters 29B, 321 (1969)
13. K.H. Schmidt, DESY Interner Bericht F 23-70/1 (1970)
14. R.J. Adler and S.D. Drell, Phys.Rev.Letters 13, 349 (1964)
15. V.Z. Jankus, Phys.Rev. 102, 1586 (1956)
16. M. Gourdin, Nuovo Cimento 28, 533 (1963), 32, 493 (E) (1964)
17. M. Gourdin, Nuovo Cimento 33, 1391 (1964)

18. M. Gourdin, Diffusion des Electrons de Haute Energie, Manon & Cie, Paris (1966)

19. F. Gross, Phys.Rev. 142, 1025 (1966), 152, 1517 (E) (1966)

20. T. Hamada and J.D. Johnston, Nucl. Phys. 34, 382 (1962)

21. G. Kessler, DESY Interner Bericht B2-68/1 (1968)

22. W. Schmidt-Parzefall, KFK 769 (1968)
S. Galster, G. Hartwig, H. Klein, J. Moritz, K.H. Schmidt, W. Schmidt-Parzefall, H. Schopper and D. Wegener, Nucl.Instr. and Meth. 76, 337 (1969)

23. S. Galster, G.Hartwig, H. Klein, J. Moritz, K.H. Schmidt, W. Schmidt-Parzefall, D. Wegener and J. Bleckwenn, KFK 963 (1969)

24. D.F. Measday and C. Richard-Serre, Cern 69-17 (1969)

25. A. Bartl and P. Urban, Fortschritte der Physik 12, 386 (1964)

26. L.W. Mo and Y.S. Tsai, Rev. of Mod. Physics 41, 205 (1969)

27. Ch. Berger, V. Burkhart, G. Knop, B. Langenbeck and K. Rith, Physikalisches Institut, Universität Bonn, Preprint 1-075, July 1969

28. H. Feshbach and E. Lomon, Rev.Mod. Phys. 39, 611 (1967)
and private communication

29. L. Huthén and M. Sugawara, Handbuch der Physik edited by S. Flügge (Springer-Verlag, Berlin, 1957) Vol. 39, p. 1

30. I. McGee, Phys.Rev. 151, 772 (1966)

31. A.O. Barut, D. Corrigan and H. Kleinert, Phys.Rev. Letters 20, 167 (1968)

32. R. Budnitz, J. Appel, L. Carroll, J. Chen, J.R. Dunning jr., Mr. Goitein, K. Hanson, D. Imrie, C. Mistretta, J.K. Walker and R. Wilson, Phys.Rev. Letters 19, 809 (1967)

TABLE I

Values of theoretical elastic electron-deuteron scattering cross sections, using various deuteron wave functions

E_o = 2500 MeV, Θ_e = 12°, q^2 = 6.5 f^{-2}

Wave function	$(\frac{d\sigma}{d\Omega})$ (cm^2/sr)
Hamada-Johnston	4.62×10^{-32}
Feshbach-Lomon	4.43×10^{-32}
Ian McGee	5.0×10^{-32}
Hulthén, no core p_D = 5 %	7.11×10^{-32}
Hulthén, core = 0.432 f, p_D = 5 %	4.69×10^{-32}
Hulthén, core = 0.561 f, p_D = 5 %	4.15×10^{-32}

TABLE II

Energy loss of protons and deuterons in plastic material

E_o (MeV)	θ_e (deg)	E_P (MeV)	$(\frac{dE}{dx})_P$ (MeV/cm)	channel (exp)	E_D (MeV)	$(\frac{dE}{dx})_D$ (MeV/cm)	channel (exp)
2500	12	137	5.9	30	71	16.8	100
2700	14	214	4.4	25	111	11.7	77
2700	15	242	4.1	23	126	10.6	63

TABLE III

List of corrections and their errors

Correction	%
Radiative correction	20. ± 2.
Dead time correction	3. ± 1.
Shower counter correction	0.5 ± 0.1

TABLE IV

Values of experimental elastic electron-deuteron scattering cross sections

Θ_e (degrees)	$\bar{\Theta}_e$ (degrees)	$\bar{q}^2$ (f^{-2})	$d\sigma/d\Omega$ (cm^2/sr)
	Set 1 : E_o = 2500 MeV		
11.2 - 11.6	11.4	6.16	$(8.11 \pm 0.41) \times 10^{-32}$
11.6 - 12.0	11.8	6.60	$(5.45 \pm 0.32) \times 10^{-32}$
12.0 - 12.4	12.2	7.04	$(4.00 \pm 0.26) \times 10^{-32}$
12.4 - 12.8	12.6	7.50	$(2.95 \pm 0.21) \times 10^{-32}$
	Set 2 : E_o = 2700 MeV		
13.0 - 13.8	13.35	9.75	$(7.54 \pm 0.54) \times 10^{-33}$
13.8 - 14.6	14.15	10.9	$(4.35 \pm 0.36) \times 10^{-33}$
	Set 3 : E_o = 2700 MeV		
14.1 - 14.45	14.25	11.03	$(3.63 \pm 0.22) \times 10^{-33}$
14.45- 14.95	14.7	11.7	$(2.68 \pm 0.16) \times 10^{-33}$
14.95- 15.35	15.15	12.42	$(2.05 \pm 0.15) \times 10^{-33}$
15.35- 15.7	15.55	13.0	$(1.56 \pm 0.13) \times 10^{-33}$

TABLE V

Sources of uncertainty in the measurement of $d\sigma/d\Omega$

Quantity	Uncertainty (%)
Density of the target	2.0
Solid angle	2.0
Electron angle	0.5
Incident electron energy	1.5
Constant of Faraday-Cup Integrator	1.0
Statistics	4.0 - 7.0

TABLE VI

Measured values of the deuteron form factor $A(q^2)$

q^2 (f^{-2})	$A(q^2)$	% error
6.16	$(9.86 \pm 0.50) \times 10^{-3}$	± 5.1
6.60	$(7.57 \pm 0.45) \times 10^{-3}$	± 5.9
7.04	$(6.40 \pm 0.41) \times 10^{-3}$	± 6.4
7.50	$(5.39 \pm 0.38) \times 10^{-3}$	± 7.0
9.75	$(2.05 \pm 0.15) \times 10^{-3}$	± 7.2
10.9	$(1.49 \pm 0.12) \times 10^{-3}$	± 8.1
11.3	$(12.87 \pm 0.78) \times 10^{-4}$	± 6.1
11.70	$(10.77 \pm 0.64) \times 10^{-4}$	± 5.9
12.42	$(9.26 \pm 0.68) \times 10^{-4}$	± 7.3
13.00	$(7.79 \pm 0.63) \times 10^{-4}$	± 8.1

TABLE VII

Values of χ^2 from a comparison of theoretical and experimental values of G_{EN}

Number of measurements: 39

wave function \ G_{EN} =	0	$-\mu_N \tau G_{EP}$	$\frac{-\mu_N \tau}{1+4\tau} G_{EP}$	$\frac{-\mu_N \tau}{1+p\tau} G_{EP}$
Feshbach-Lomon	275	214	33.6	29.3 (p = 5.6)
Hamada-Johnston	196	399	84.8	39.7 (p = 10.7)
McGee	106	495	141.5	35.7 (p = 19.7)
Hulthén (no core)	438	2716	1537.3	534.3 (p >100.)
Hulthén (core, 0.432 f)	786	123	305.0	60.2 (p = -1.7)
Hulthén (core, 0.561 f)	1034	218	433.5	158.9 (p = -1.3)

TABLE VIII

Measured values of the isoscalar electric form factor G_{ES}

q^2 (f^{-2})	wave function of Hamada-Johnston	wave function of Lomon-Feshbach
6.16	0.297 ± 0.008	0.297 ± 0.008
6.60	0.280 ± 0.009	0.281 ± 0.009
7.04	0.277 ± 0.009	0.278 ± 0.009
7.50	0.276 ± 0.010	0.278 ± 0.010
9.75	0.235 ± 0.009	0.239 ± 0.009
10.90	0.225 ± 0.010	0.231 ± 0.010
11.03	0.209 ± 0.007	0.215 ± 0.007
11.70	0.205 ± 0.007	0.212 ± 0.007
12.42	0.203 ± 0.008	0.211 ± 0.008
13.00	0.195 ± 0.009	0.204 ± 0.009

Figure Captions

Fig. 1 The differential cross section as a function of the neutron form factor G_{EN}, using the formula of Gourdin[17] and the wave function of Hamada-Johnston[20]

Fig. 2 Contributions to $A(q^2)$ from terms involving the electric, the magnetic, and the quadrupole form factor. The same theoretical predictions as in Fig. 1 are used. G_{EN} is set equal to zero.

Fig. 3 Relativistic corrections in % to $A(q^2)$ as taken from Gross[19] using the Hamada-Johnston[20] wave function.

Fig. 4 Experimental setup.

Fig. 5 Pulse height spectrum of the deuteron-counter.

Fig. 6 Electron spectra (at the right) as a function of the threshold in the pulse height spectrum (at the left), shown for three thresholds.

Fig. 7 Number of events from the elastic electron-deuteron scattering as a function of the threshold in the pulse height spectrum of the deuteron-counter.

Fig. 8 Electron spectra from the elastic electron-deuteron scattering in 0.4° intervals of the electron scattering angle.

Fig. 9 Measured values of the quantity $A(q^2)$, and theoretical predictions of the formula of Gross[19], using the wave function of Hamada-Johnston[20](———), Feshbach-Lomon[28](— —), McGee[30] (-----), Hulthén[29] (— ···), Hulthén with a core at 0.432 f (— ··), and Hulthén with a core at 0.561 f (—— ·). G_{EN} is set equal to zero.

Fig. 10 The deuteron form factor $A(q^2)$ using the formula of Gross[19] and the wave function of Hamada-Johnston[20]. G_{EN} is varied from -0.05 to +0.05.

Fig. 11 The measured electric neutron form factor G_{EN}, when using the formula of Gross[19], the four-pole fit[27] for the electric proton form factor G_{EP} and the wave function of Hamada-Johnston[20]. The dashed and dashdot curves are the predictions $G_{EN} = -\mu_N \tau G_{EP}$[31] and $G_{EN} = -\mu_N \tau/(1+4\tau)\cdot G_{EP}$[32]. The solid curve represents the prediction $G_{EN} = -\mu_N \tau/(1+p\tau)\cdot G_{EP}$ with p = 10.7.

Fig. 12 The measured electric neutron form factor G_{EN}, when using the wave function of McGee[30]. The solid curve is the prediction $G_{EN} = -\mu_N \tau/(1+p\tau)\cdot G_{EP}$ with p = 19.7. See caption to Fig. 11.

Fig. 13 The measured electric neutron form factor G_{EN}, when using the wave function of Feshbach-Lomon[28]. The solid curve is the prediction $G_{EN} = -\mu_N \tau/(1+p\tau)\cdot G_{EP}$ with p = 5.6. See caption to Fig. 11.

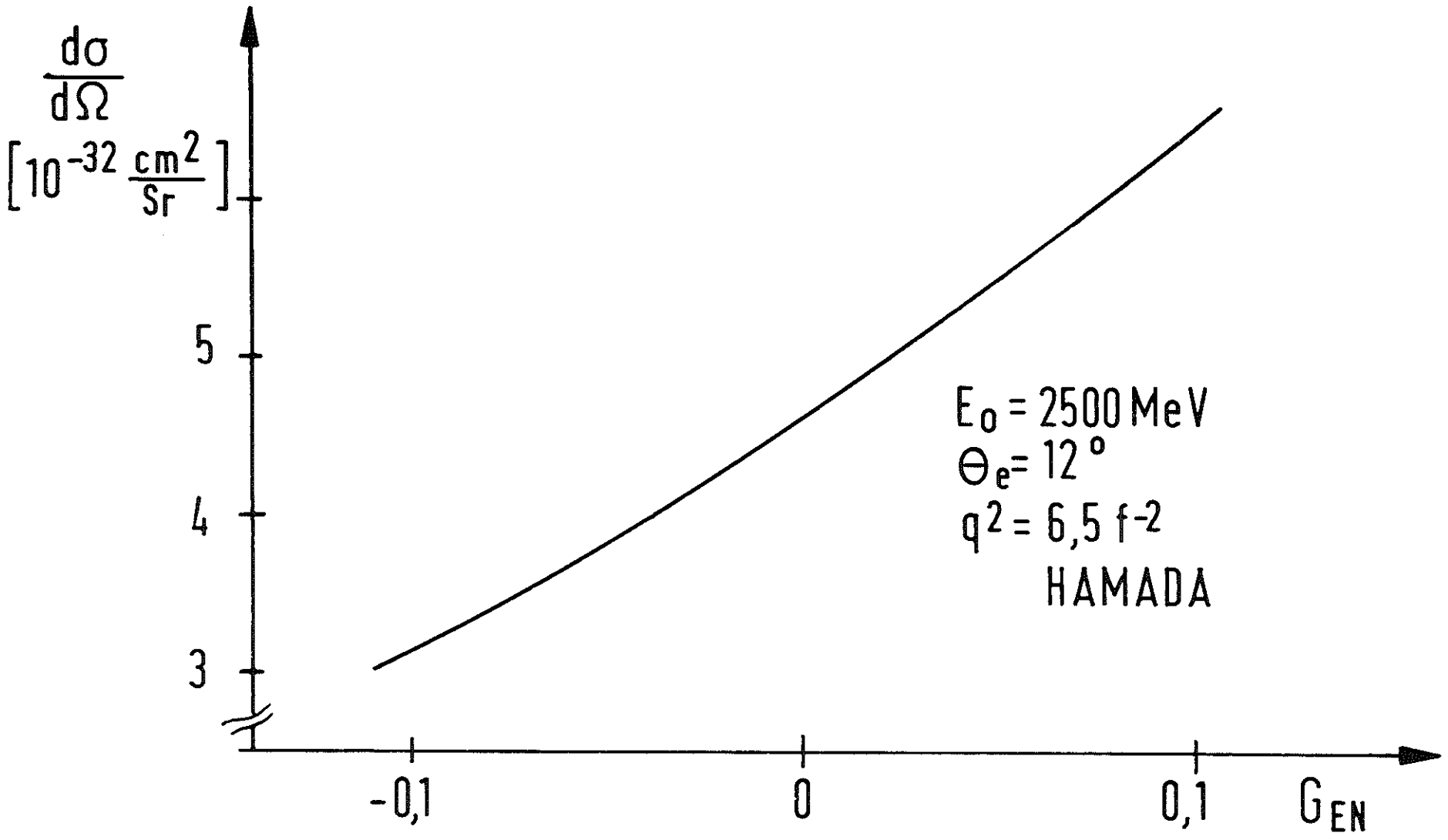

Fig. 1

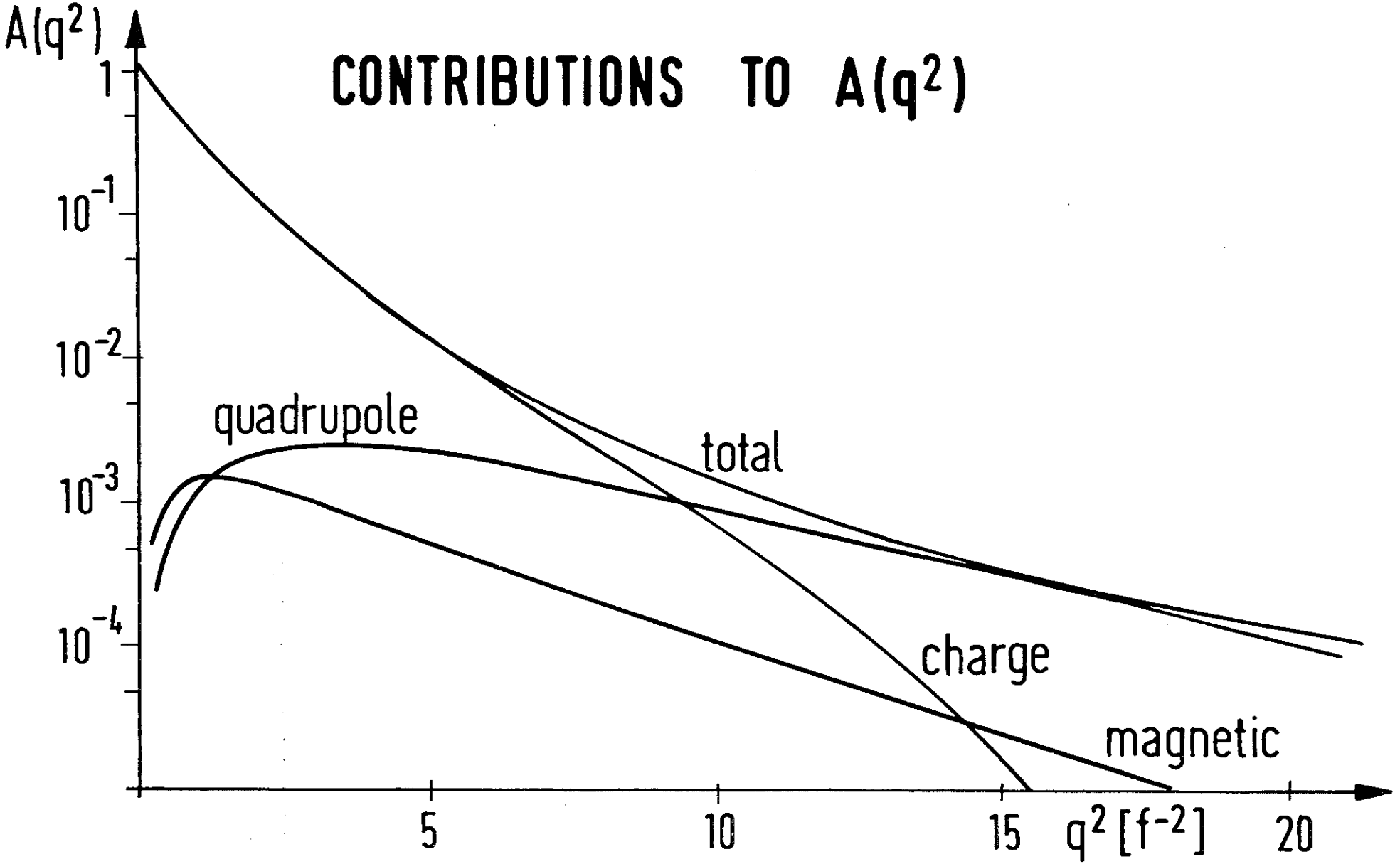
CONTRIBUTIONS TO A(q²)
A(q²)
1
10⁻¹
10⁻²
10⁻³
10⁻⁴
quadrupole
total
charge
magnetic
5
10
15
q² [f⁻²]
20

Fig. 2

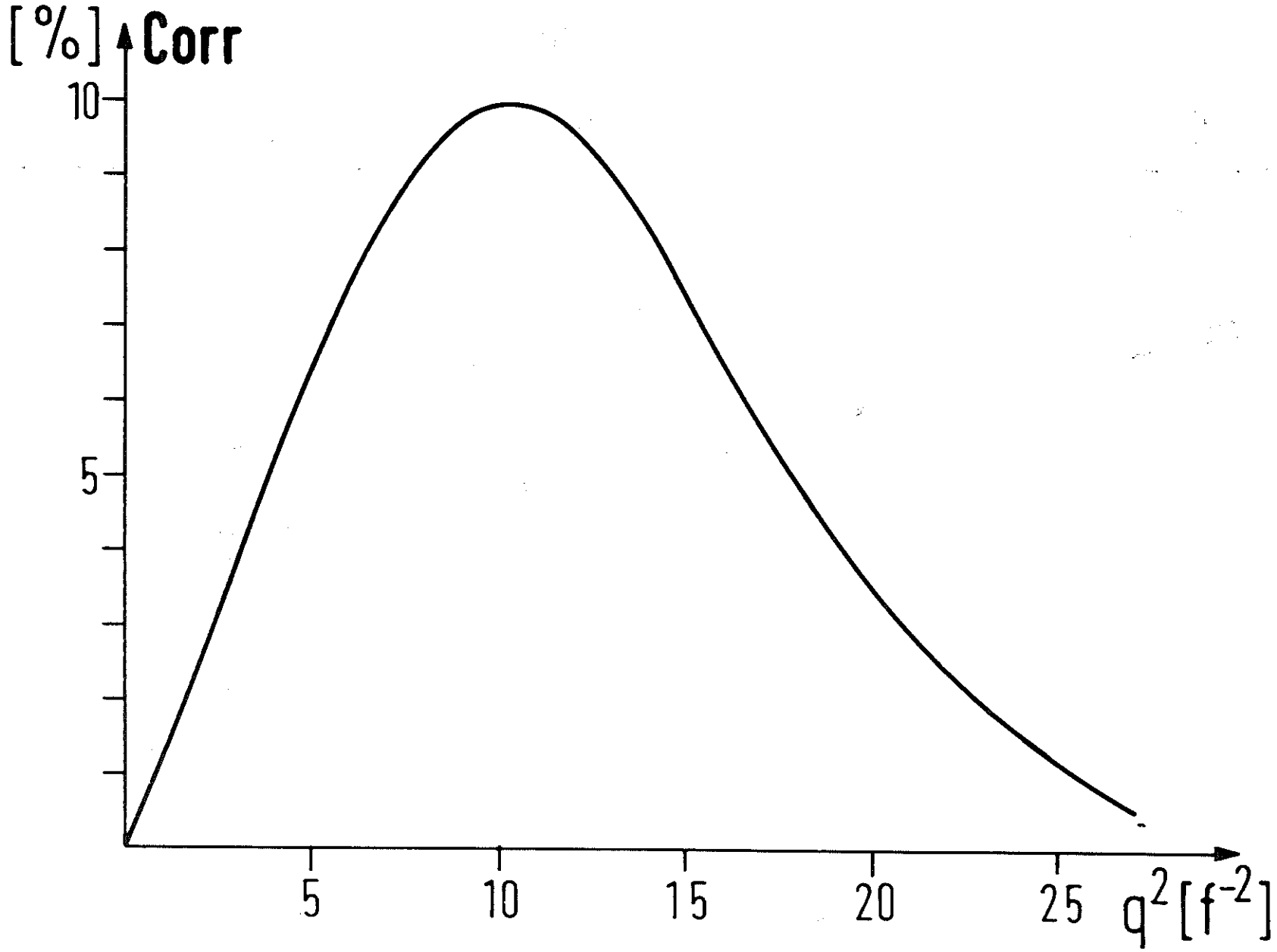

Fig. 3

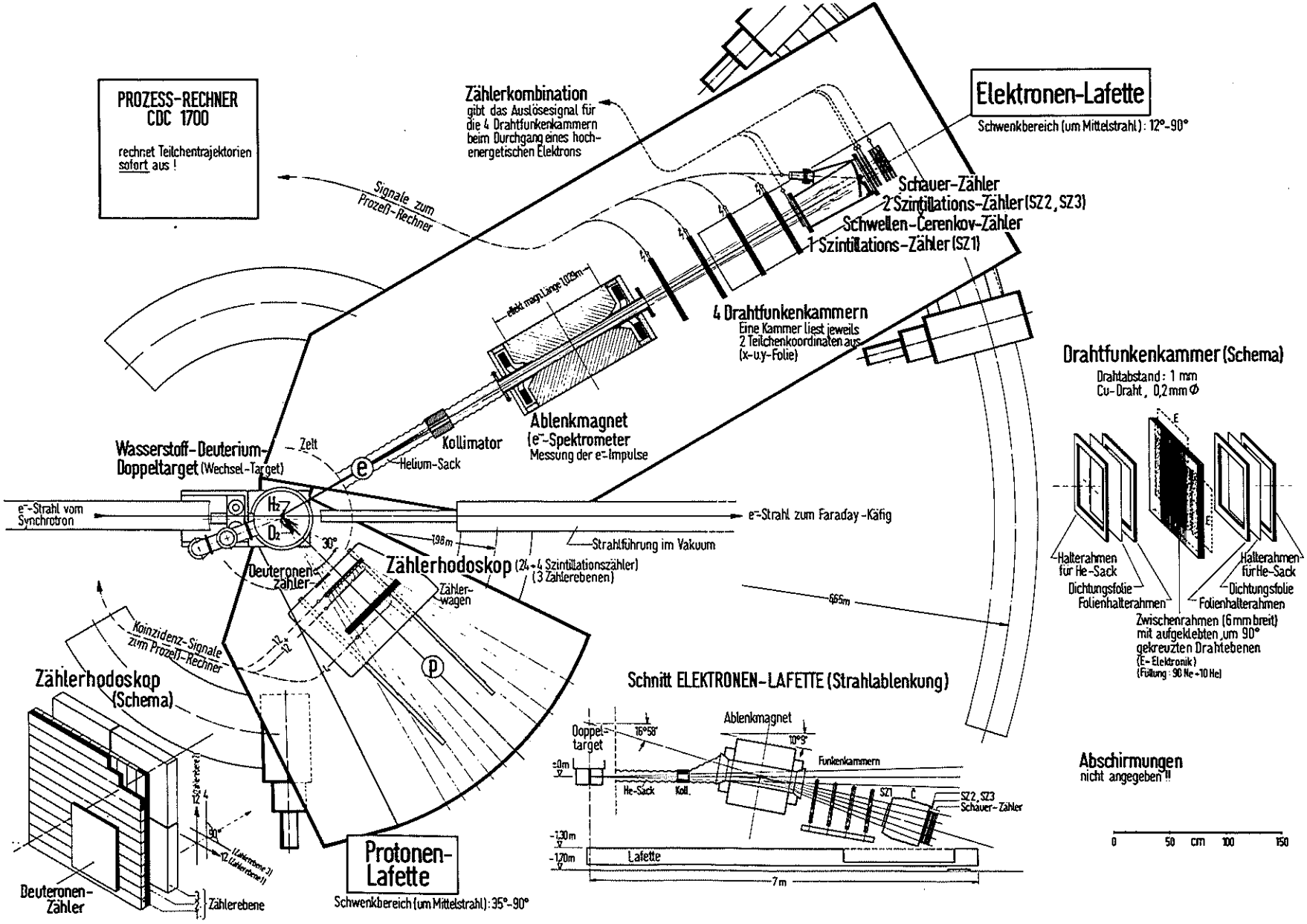
PROZESS-RECHNER
CDC 1700
rechnet Teilchentrajektorien sofort aus !
Signale zum Prozeß-Rechner
Zählerkombination
gibt das Auslösesignal für die 4 Drahtfunkenkammern beim Durchgang eines hochenergetischen Elektrons
Elektronen-Lafette
Schwenkbereich (um Mittelstrahl): 12°-90°
Schauer-Zähler
2 Szintillations-Zähler (SZ2, SZ3)
Schwellen-Cerenkov-Zähler
1 Szintillations-Zähler (SZ1)
4 Drahtfunkenkammern
Eine Kammer liest jeweils 2 Teilchenkoordinaten aus (x-u,y-Folie)
eff. magn. Länge 1,02m
Ablenkmagnet
(e⁻-Spektrometer
Messung der e⁻-Impulse
Kollimator
Helium-Sack
Zelt
Wasserstoff-Deuterium-Doppeltarget (Wechsel-Target)
e⁻-Strahl vom Synchrotron
e⁻-Strahl zum Faraday-Käfig
Strahlführung im Vakuum
1,98m
6,65m
30°
Deuteronen-Zähler
Zählerhodoskop (24+4 Szintillationszähler) (3 Zählerebenen)
Zähler-wagen
Koinzidenz-Signale zum Prozeß-Rechner
Zählerhodoskop (Schema)
Deuteronen-Zähler
Zählerebene
Protonen-Lafette
Schwenkbereich (um Mittelstrahl): 35°-90°
Schnitt ELEKTRONEN-LAFETTE (Strahlablenkung)
Doppel-target
Ablenkmagnet
16°58'
10°9'
Funkenkammern
He-Sack
Koll.
SZ1
C
SZ2, SZ3 Schauer-Zähler
Lafette
7m
Drahtfunkenkammer (Schema)
Drahtabstand: 1 mm
Cu-Draht, 0,2 mm Ø
Halterahmen für He-Sack
Dichtungsfolie
Folienhalterahmen
Zwischenrahmen (6 mm breit) mit aufgeklebten, um 90° gekreuzten Drahtebenen
(E-Elektronik)
(Füllung: 90 Ne +10 He)
Abschirmungen
nicht angegeben !!
0
50 cm
100
150

Fig. 4

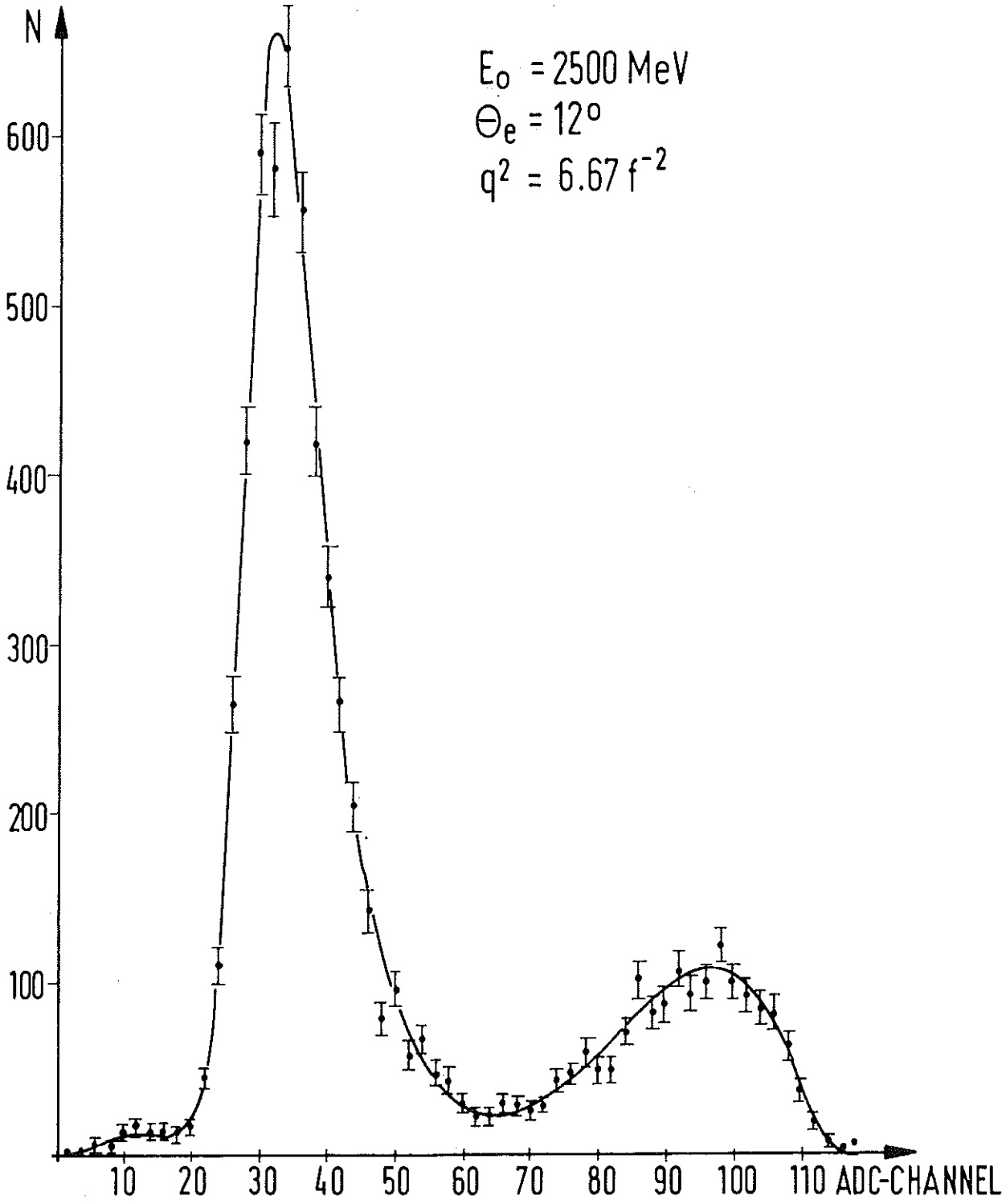
N
600
500
400
300
200
100
E_o = 2500 MeV
Θ_e = 12°
q^2 = 6.67 f^{-2}
10
20
30
40
50
60
70
80
90
100
110 ADC-CHANNEL

Fig. 5

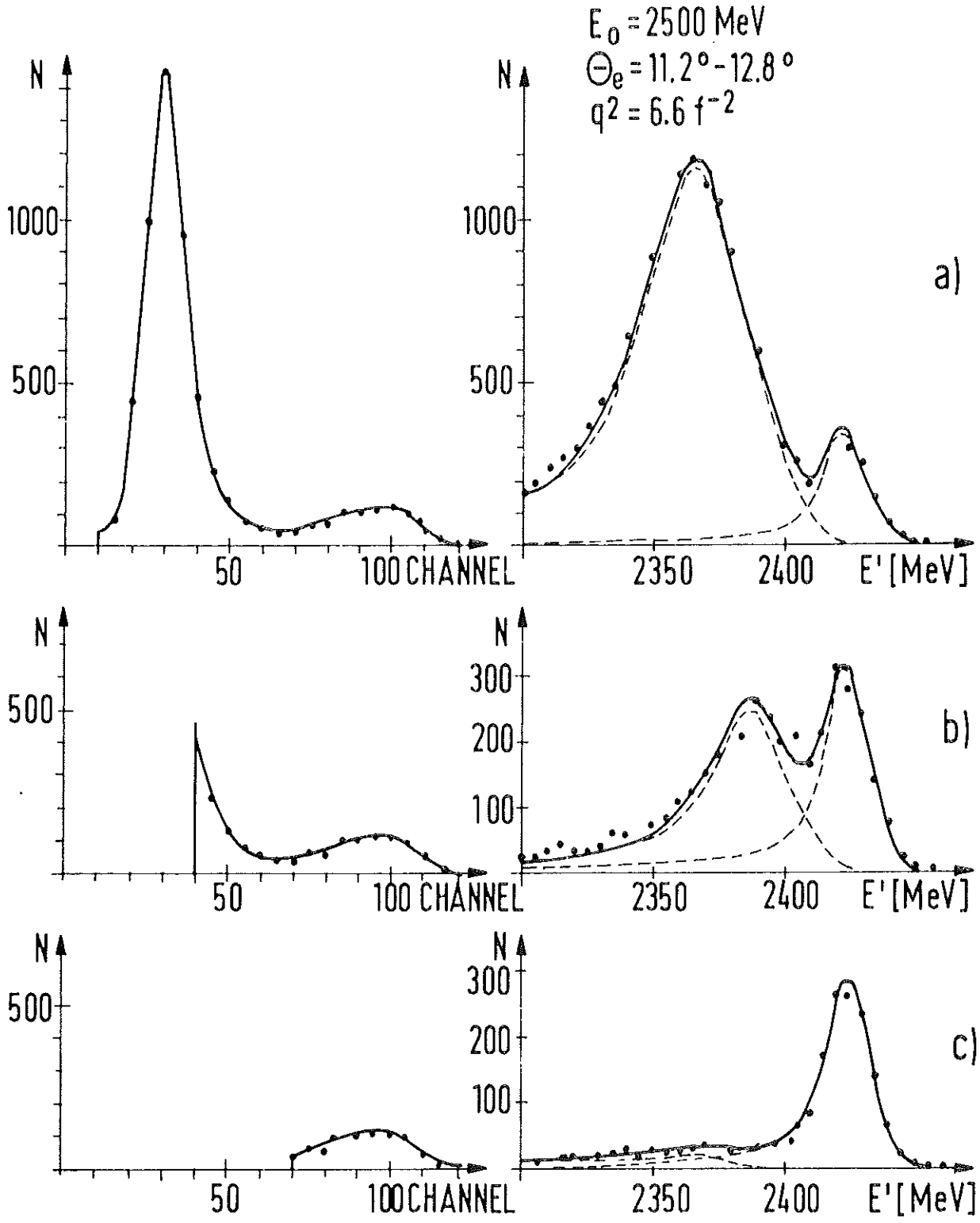
$E_0 = 2500$ MeV
$\Theta_e = 11.2° - 12.8°$
$q^2 = 6.6\ f^{-2}$
N
1000
500
50
100 CHANNEL
2350
2400
E' [MeV]
a)
300
200
100
b)
c)

Fig. 6

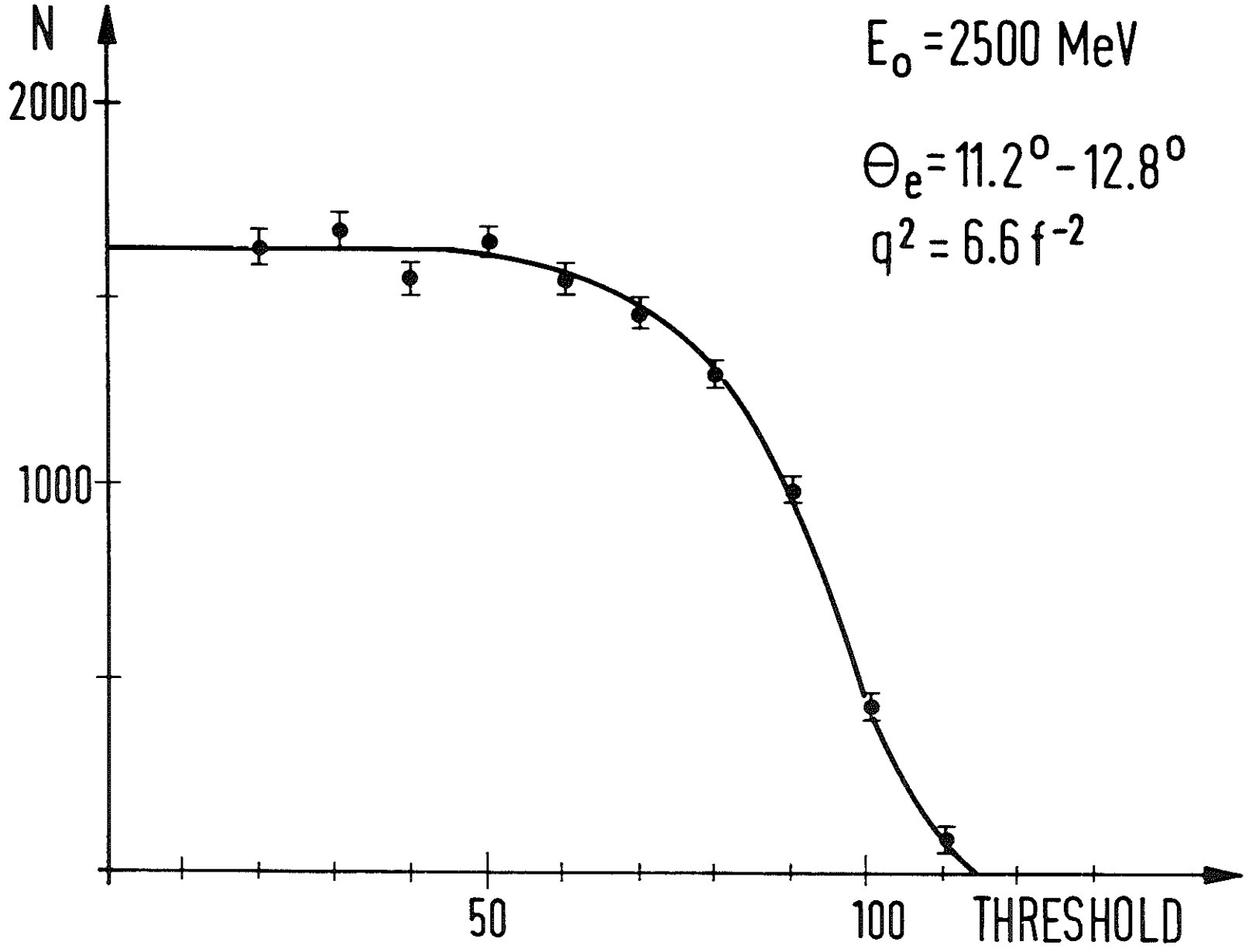
N
2000
1000
E_o = 2500 MeV
Θ_e = 11.2° - 12.8°
q^2 = 6.6 f^{-2}
50
100
THRESHOLD

Fig. 7

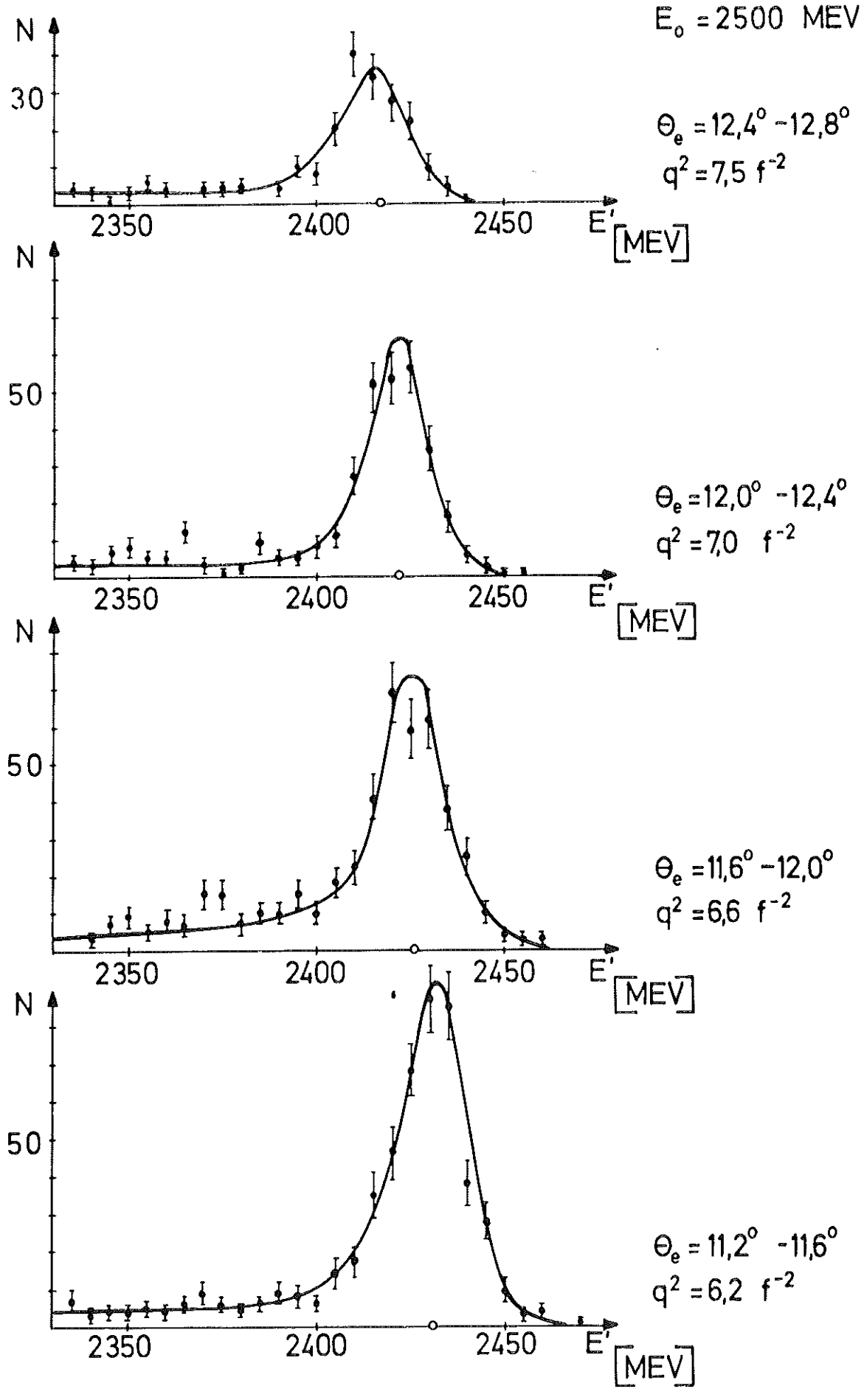
N
30
2350
2400
2450
E'
[MEV]
E_0 = 2500 MEV
Θ_e = 12,4° - 12,8°
q^2 = 7,5 f^{-2}
N
50
2350
2400
2450
E'
[MEV]
Θ_e = 12,0° - 12,4°
q^2 = 7,0 f^{-2}
N
50
2350
2400
2450
E'
[MEV]
Θ_e = 11,6° - 12,0°
q^2 = 6,6 f^{-2}
N
50
2350
2400
2450
E'
[MEV]
Θ_e = 11,2° - 11,6°
q^2 = 6,2 f^{-2}

Fig. 8

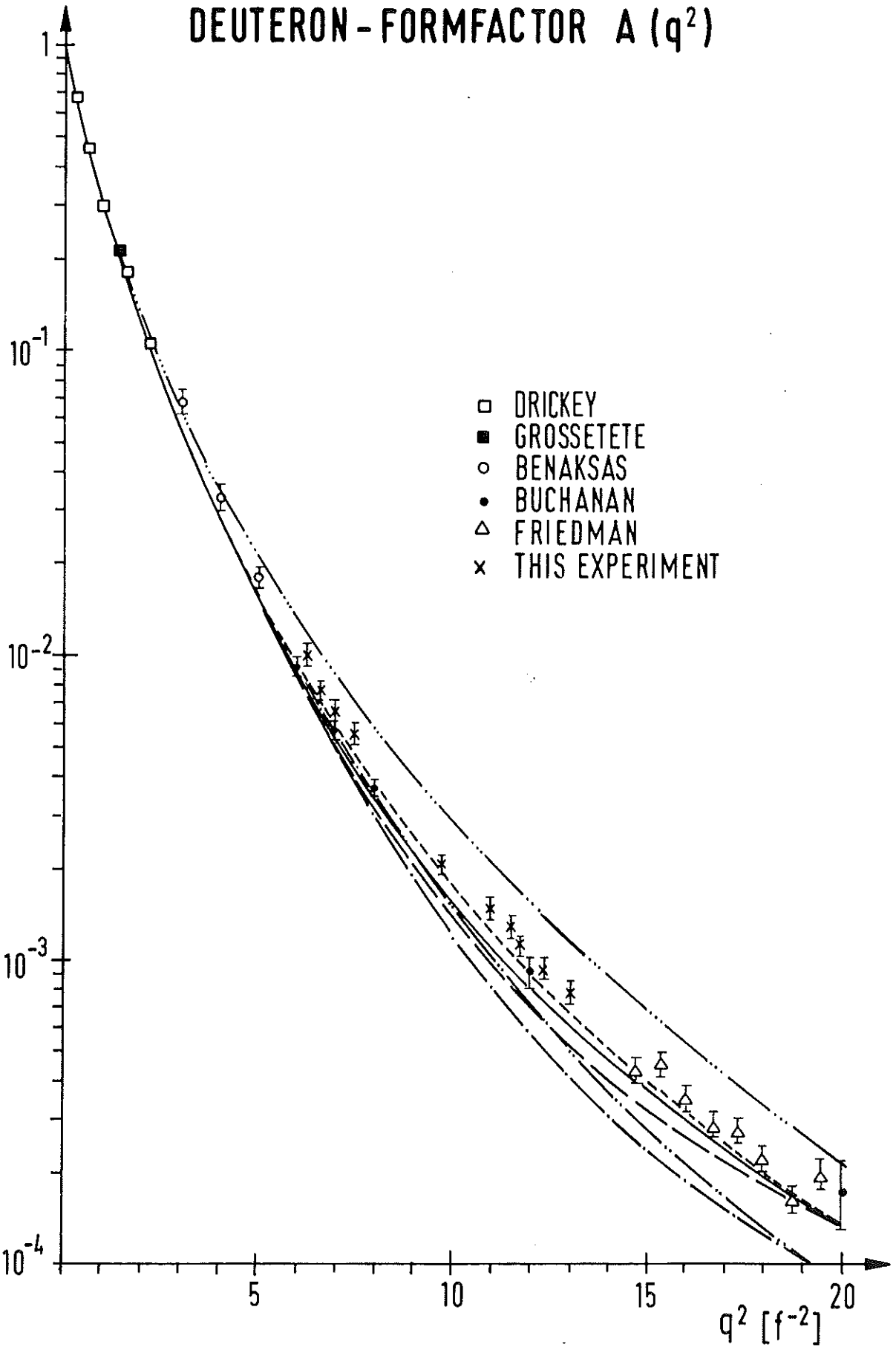
DEUTERON-FORMFACTOR A(q²)
1
10⁻¹
10⁻²
10⁻³
10⁻⁴
5
10
15
20
q² [f⁻²]
DRICKEY
GROSSETETE
BENAKSAS
BUCHANAN
FRIEDMAN
THIS EXPERIMENT

Fig. 9

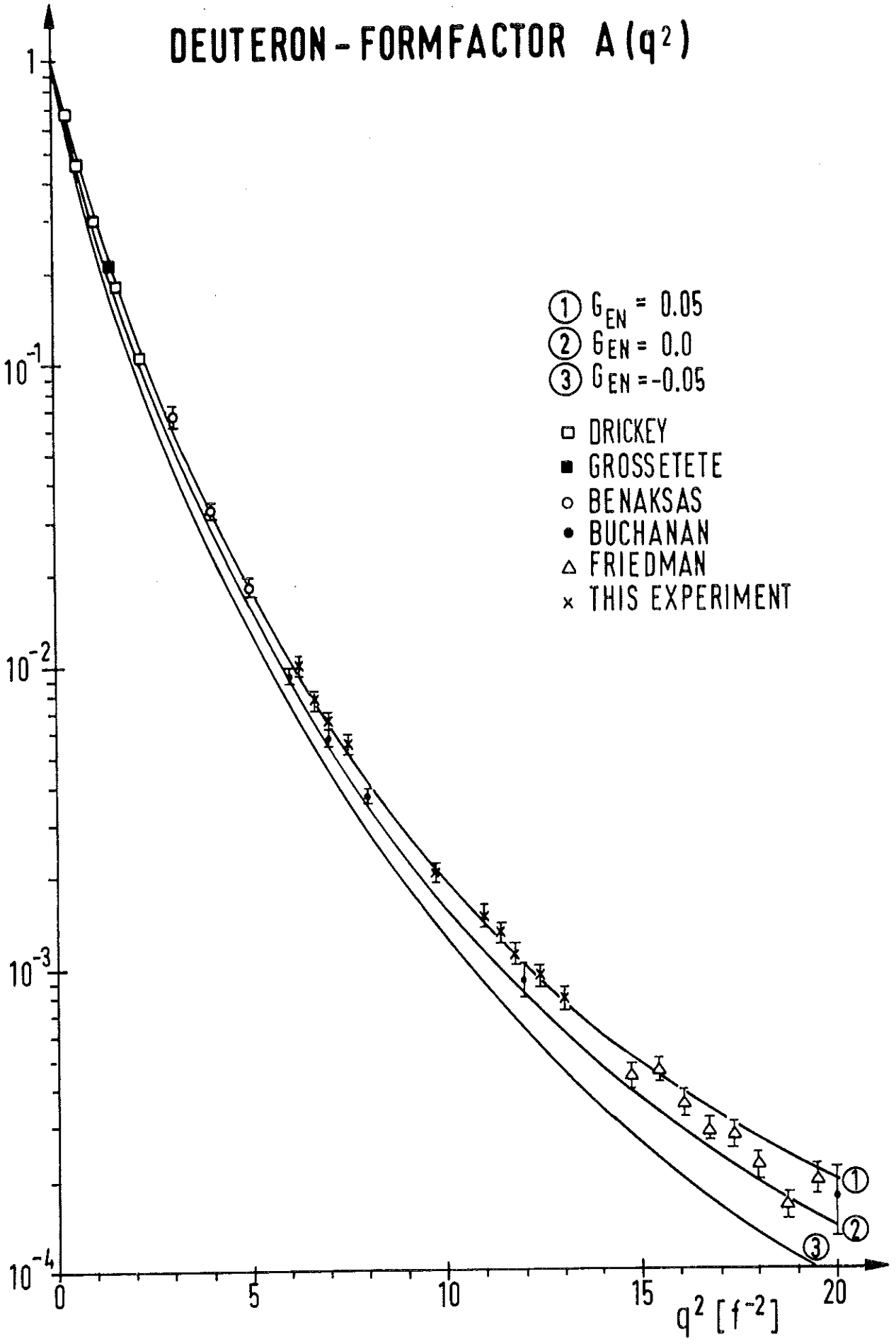
DEUTERON-FORMFACTOR A(q²)
1
10⁻¹
10⁻²
10⁻³
10⁻⁴
0
5
10
15
20
q² [f⁻²]
① G_EN = 0.05
② G_EN = 0.0
③ G_EN = -0.05
DRICKEY
GROSSETETE
BENAKSAS
BUCHANAN
FRIEDMAN
THIS EXPERIMENT

Fig. 10

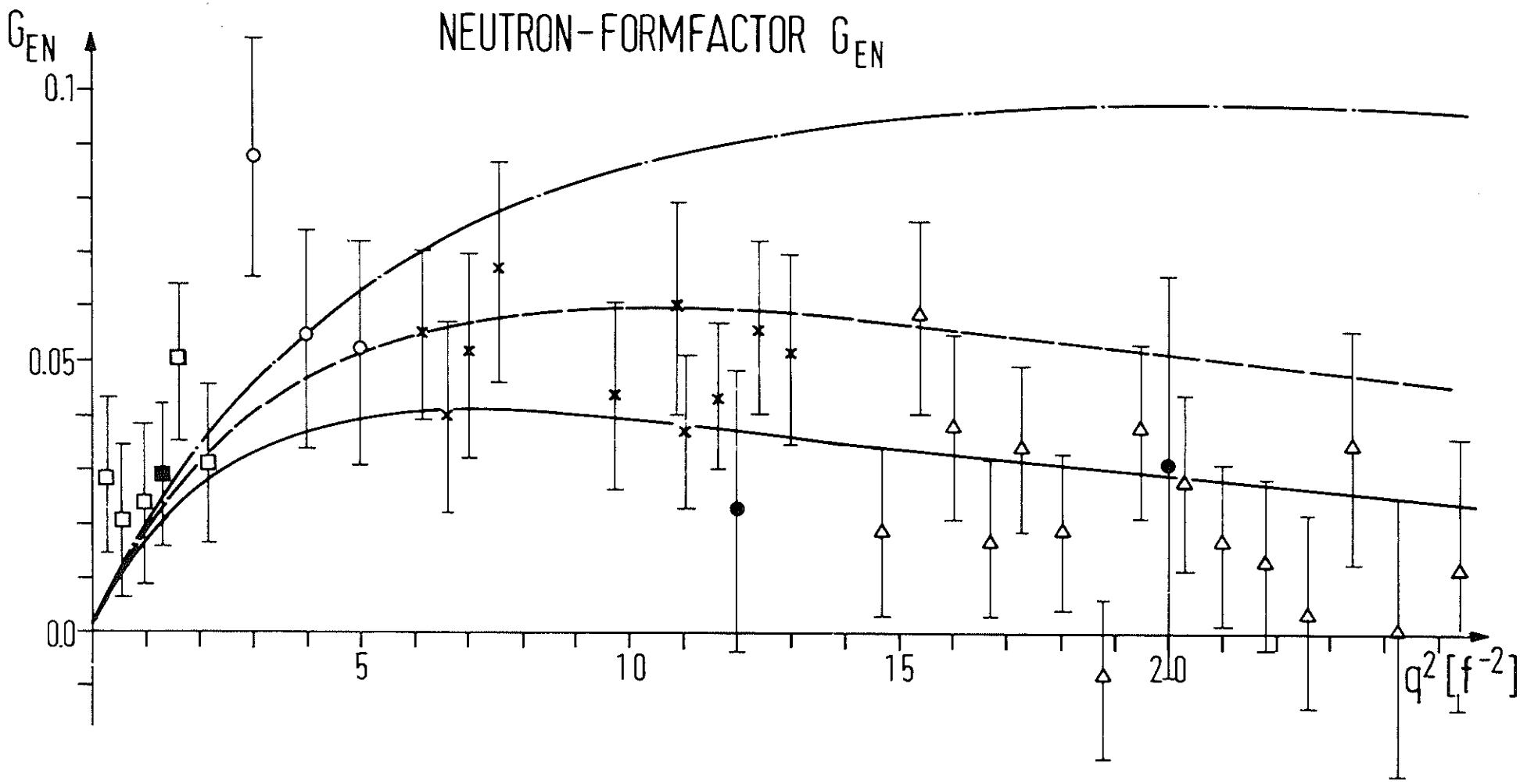

Fig. 11

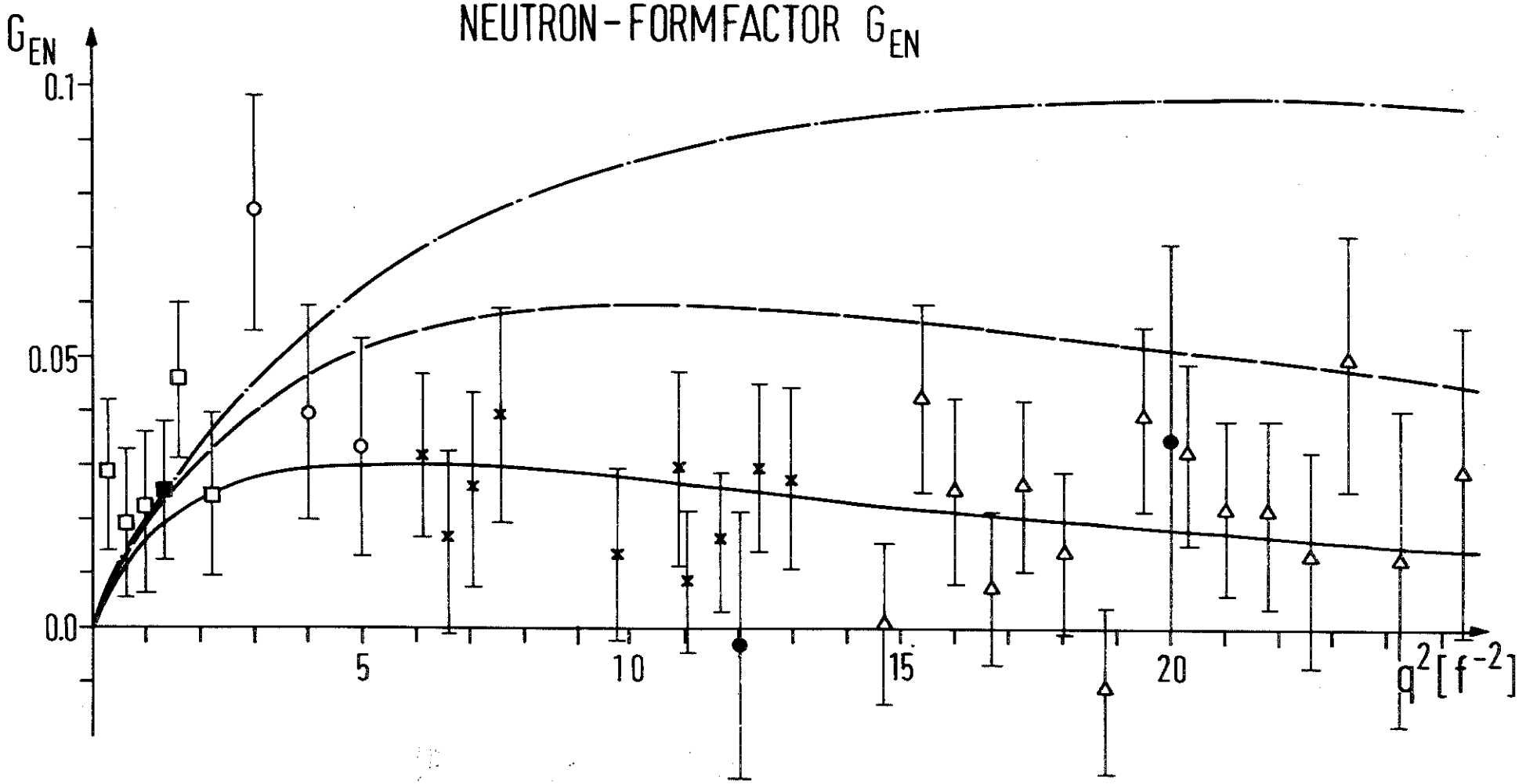

Fig. 12

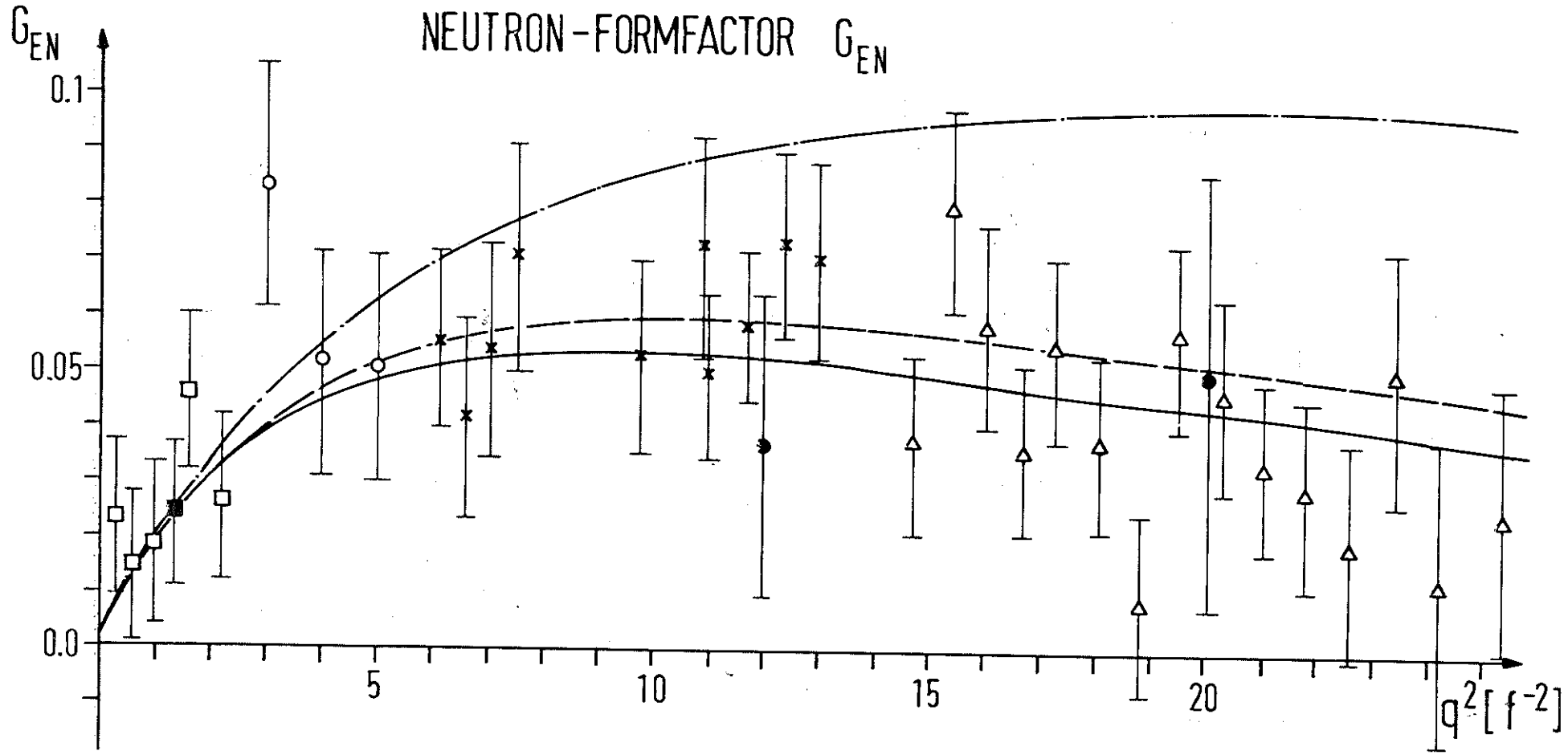

Fig. 13